Journal of Controlled Release 287 (2018) 156–166

Contents lists available at ScienceDirect

Journal of Controlled Release

journal homepage: www.elsevier.com/locate/jconrel

Dopamine-loaded blood exosomes targeted to brain for better treatment of Parkinson's disease

Mengke Qu[a], Qing Lin[a], Luyi Huang[b], Yao Fu[a], Luyao Wang[a], Shanshan He[a], Yu Fu[a], Shengyong Yang[b], Zhirong Zhang[a], Ling Zhang[c,*], Xun Sun[a,*]

[a] Key Laboratory of Drug Targeting and Drug Delivery Systems of Ministry of Education, West China School of Pharmacy, Sichuan University, Chengdu 610041, China
[b] The State Key Laboratory of Biotherapy/Collaborative Innovation Center, West China Hospital, Sichuan University, Chengdu 610041, China
[c] College of Polymer Science and Engineering, Sichuan University, Chengdu 610065, China

ARTICLE INFO

Keywords:
Blood exosomes
Brain targeting
Mechanism of targeting
Drug delivery
Parkinson's disease

ABSTRACT

Parkinson's disease (PD), one of the most common movement and neurodegenerative disorders, is challenging to treat, largely because the blood-brain barrier blocks passage of most drugs. Here we find exosomes from blood showing natural brain targeting ability which involved the transferrin-transferrin receptor interaction. Thus, we develop a biocompatible platform based on blood exosomes for delivering drugs across the blood-brain barrier. Blood exosomes show sizes between 40 and 200 nm and spherical morphology, and dopamine can be efficiently loaded into blood exosomes by a saturated solution incubation method. Further *in vitro* and *in vivo* studies demonstrates these exosomes successfully delivered dopamine to brain, including the striatum and substantia nigra. Brain distribution of dopamine increased > 15-fold by using the blood exosomes as delivery system. Dopamine-loaded exosomes show much better therapeutic efficacy in a PD mouse model and lower systemic toxicity than free dopamine after intravenous administration. These results suggest that blood exosomes can be used as a promising drug delivery platform for targeted therapy against PD and other diseases of the central nervous system.

1. Introduction

Parkinson's disease (PD), which affects primarily the motor system, is the second most common neurodegenerative disorder with over 6.2 million cases and 117,400 deaths around the world annually [1]. Incidence and mortality are expected to increase as the global population ages. The major cause of PD is thought to be the loss of dopaminergic substantia nigra neurons and formation of α-synuclein-containing Lewy bodies [2]. PD is often treated by administering dopamine, but delivering it efficiently to the brain is challenging because of the blood-brain barrier (BBB). To improve brain distribution, dopamine can be encapsulated in drug delivery systems, such as ligand-modified nanoparticles, micelles and dendrimers [3], which have achieved modest success to overcome BBB. However, what partly impedes the regulatory approval for clinical use of nanomaterials is their biocompatibility and ligand modification increases the production cost and complexity of vehicles. Alternatively, the dopamine precursor levodopa can cross the BBB better than dopamine, whereas only 1% given levodopa could reach the brain due to the presence of abundant levodopa decarboxylase in plasma [4] and it must be converted to dopamine in the brain by the decarboxylase, which is less active in the brain of patients with PD [5].

Therefore, we aimed to design a novel drug delivery system that would allow the direct use of dopamine and cross the BBB effectively with maximum biocompatibility and minimum toxicity. We focused on exosomes, which are spherical endogenous vesicles (40–200 nm) [6], with low immunogenicity and excellent biocompatibility that are derived from the luminal membranes of multivesicular bodies and are constitutively released by fusion with the cell membrane [7]. Exosomes have already been explored as drug delivery vehicles [8]. For example, small-molecule therapeutics such as doxorubicin, paclitaxel and curcumin have been encapsulated into exosomes to treat cancer and inflammatory disease [9–11]. Exosomes have also been loaded with human Mucin 1 protein or micro RNA let-7a for cancer therapy [12,13]. Addition of transgenes to the cells from which exosomes are obtained allows the production of exosomes carrying, for example, fusions of membrane proteins with iRGD peptides or RVG, which can target tumors or the brain [9,14,15]. However, this transgene-based approach for targeting is complex, and success is not guaranteed. Besides, exosomes derived from different cell lines were shown to deliver drug to

* Corresponding authors.
E-mail addresses: femcivrogner@gmail.com (L. Zhang), sunxun@scu.edu.cn (X. Sun).

https://doi.org/10.1016/j.jconrel.2018.08.035
Received 12 June 2018; Received in revised form 20 August 2018; Accepted 25 August 2018
Available online 27 August 2018
0168-3659/

the brain through the nose, but isolating sufficient exosomes from cells proved difficult, and intranasal administration often could not give enough dose within a single treatment for patients [16].

In order to find an approach to acquire abundant exosomes, exosomes derived from blood were taken into consideration because plenty of blood exosomes were released by reticulocytes during their maturation to erythrocytes vesicles [17]. Our experiments also further demonstrated that blood exosomes without any modification had a good natural targeting ability to brain.

Herein, we developed a blood exosome platform for brain-targeted drug delivery against PD. We isolated exosomes from mouse blood and characterized them. Then, we confirmed the natural brain targeting abilities of blood exosomes *in vitro* and *in vivo* and elucidated the mechanism of brain targeting. Afterwards, dopamine was incorporated into blood exosomes and its *in vivo* biodistribution was investigated. We further evaluated therapeutic outcome of dopamine-loaded blood exosomes in a mouse model of PD. These results revealed the potential of blood exosomes for the targeted brain delivery of drugs against PD and other diseases of the central nervous system.

2. Material and methods

2.1. Isolation and characterization of blood exosomes

Blood samples were collected from the orbit venous plexus of Kunming mice to acquire fresh serum rather than taking blood by sacrificing them. Fresh serum was centrifugated at 12,000 ×*g*, filtrated through 0.22 μm filter, and centrifugated again at 200,000 ×*g*. Blood exosomes were acquired by taking the pellet. Blood exosomes was incubated with saturated solution of dopamine with 0.02% ascorbic acid for 24 h at room temperature, then ultracentrifugation was used to remove free dopamine and phosphate buffer solution (PBS) was selected to clean dopamine-loaded blood exosomes again. Afterwards, dopamine encapsulated in blood exosomes was extracted into acetonitrile of 0.02% ascorbic acid. Liquid chromatography followed by tandem mass spectrometry (LC-MS/MS) (Agilent 6410B, USA) was used to measure the quantity of dopamine encapsulated in blood exosomes; the amount of blood exosomes was quantified by a micro BCA assay (Thermo Fisher Scientific, Waltham, Massachusetts, USA). The drug-loading rate was calculated (drug-loading rate (%) = The quantity of dopamine encapsulated / The total quantity of dopamine encapsulated and blood exosomes × 100).

The morphology of blood exosomes was examined by transmission electron microscopy (TEM, Hitachi H-600, Japan). Tunable Resistive Pulse Sensing (Izon Science, New Zealand) was used to assess particle sizes and the number of blood exosomes. Next, the levels of CD9, CD63, CD81 and TfR expression on blood exosomes were measured by western blotting.

2.2. Mechanism of cellular uptake

When investigating the impact of transferrin on cellular uptake of blood exosomes by bEnd.3 cells, cells were respectively pretreated with 40, 80 and 160 μg/mL of transferrin for 30 min at 37 °C. Alternatively, PHK67-labeled blood exosomes (100 μg/mL) were respectively pretreated with 40, 80 and 160 μg/mL of transferrin for 4 h at 4 °C. The exosomes derived from Hela and DC 2.4 cells were used as the negative and the positive control respectively. bEnd.3 cells were pretreated with 160 μg/mL of transferrin for 30 min at 37 °C; or PHK67-labeled Hela exosomes or DC 2.4 exosomes (100 μg/mL) were respectively pretreated with 40, 80 and 160 μg/mL of transferrin for 4 h at 4 °C. Hela cells as the negative control were respectively pretreated with 40, 80 and 160 μg/mL of transferrin for 30 min at 37 °C; or PHK67-labeled blood exosomes (100 μg/mL) were pretreated with 160 μg/mL of transferrin for 4 h at 4 °C.

2.3. Exploring the form of transferrin

Transferrin solution (10 mg/mL) was incubated for 4 h at 4 °C or 37 °C. The equal amount of transferrin was added into tricine-polyacrylamide or tricine-SDS-polyacrylamide gel respectively. When gel electrophoresis was finished, coomassie blue R250 was used to stain protein for 90 min at room temperature.

2.4. Qualitative analysis of dopamine distribution

Dopamine-loaded blood exosomes or free dopamine (dopamine dose of 18 mg/kg) were injected into the Kunming mice intravenously. 6 h after the administration, mice of each group (n = 5) were treated with heart perfusion; the blood plasma and tissues (heart, liver, spleen, lung, kidney, brain) were quickly collected. The dopamine concentrations of different tissues and blood plasma were measured by LC-MS/MS [18]. Meanwhile, sterile 0.9% saline was intravenously injected into mice as control.

2.5. Distribution in the mice brain

DiD-labeled blood exosomes (10 mg/kg) or the equal amount of free DiD were injected into the Kunming mice intravenously. 6 h after the administration, mice were treated with heart perfusion, then brains were removed and frozen in optimal cutting temperature embedding medium (Sakura, Torrance, CA, USA) at −80 °C. Frozen sections of 10 mm in thickness were prepared with a cryotome cryostat (CM1950, Leica, Germany) and stained with 300 nM DAPI at room temperature. Then the sections of striatum, substantia nigra and hippocampus were immediately imaged under the fluorescence microscope (Axiovert40 CFL, Zeiss, Germany). Meanwhile, sterile 0.9% saline was also intravenously injected into mice as control.

2.6. Therapeutic efficacy for PD

Kunming mice were randomly divided into 6 groups (n = 12) and given with different treatments respectively (Table 1). After three weeks, mice were treated with heart perfusion and brains were

Table 1
Treatments for Kunming mice in different groups.

Groups	Treatments
Control	Sham, i.v. injection of 0.2 mL N.S.[a] at an interval of 1 day for ten times
1	6-OHDA lesion, i.v. injection of 0.2 mL N.S.[a] at an interval of 1 day for ten times
2	6-OHDA lesion, i.v. injection of 0.2 mL blood-exo[b] at an interval of 1 day for ten times
3	6-OHDA lesion, i.v. injection of 0.2 mL levodapa (equivalent to 4.95 mg/kg body weight per time) at an interval of 1 day for ten times
4	6-OHDA lesion, i.v. injection of 0.2 mL dopamine (equivalent to levodapa 4.95 mg/kg body weight per time) at an interval of 1 day for ten times
5	6-OHDA lesion, i.v. injection of 0.2 mL DA-blood-exo[c] (equivalent to levodapa 4.95 mg/kg body weight per time) at an interval of 1 day for ten times

[a] Sterile 0.9% saline.
[b] Unloaded blood exosomes.
[c] Dopamine-loaded blood exosomes.

Table 2
Treatments for Kunming mice in 3 different groups.

Groups	Treatments
Control	i.v. injection of 0.2 mL N.S.[a] at an interval of 1 day for ten times
1	i.v. injection of 0.2 mL dopamine (equivalent to levodapa 4.95 mg/kg body weight per time) at an interval of 1 day for ten times
2	i.v. injection of 0.2 mL DA-blood-exo[b] (equivalent to levodapa 4.95 mg/kg body weight per time) at an interval of 1 day for ten times

[a] Sterile 0.9% saline.
[b] Dopamine-loaded blood exosomes.

removed. The level of lesioned striatal dopamine was measured by LC-MS/MS; the activity of striatal tyrosine hydroxylase was evaluated by immunohistochemistry; and oxidative stress level of each group was measured according to the manufacturer's instructions. Glutathione peroxidase, total superoxide dismutase, catalase, and total antioxidant capacity reagent kits (Jiancheng, Nanjing, China) were used to measure the glutathione, enzymatic antioxidants (total superoxide dismutase and catalase), and total antioxidant capacity of lesioned striatum respectively.

2.7. In vivo toxicity of dopamine-loaded blood exosomes

Kunming mice were randomly divided into 3 groups ($n = 5$) and given different treatments respectively (Table 2). After three weeks, organs (heart, liver, spleen, lung, kidney, brain) were isolated for Hematoxylin-Eosin staining and examined under microscope (BX53, Olympus, Japan). A series of physiological indexes, such as creatine kinase, aspartate aminotransferase, alanine aminotransferase, urea nitrogen and serum creatinine, were monitored using a biochemistry analyzer (Hitachi7020,Japan).

2.8. Statistical analysis

Statistical analysis was conducted using GraphPad Prism software (Version 6.01). Statistical comparisons were performed by one-way ANOVA (Dunnett's multiple comparisons test) for multiple groups, except for Supplementary Fig. S4B-D which were performed by two-way ANOVA; $P < .05$, $P < .01$ and $P < .001$ were respectively considered indications as statistically different, significantly different and very significantly different.

3. Results and discussion

3.1. Isolation and characterization of blood exosomes

The modified ultracentrifugation method described above was used to purify exosomes from the serum. The larger molecular weight proteins are precipitated by 12,000 ×*g* centrifugation and supernatant is collected. With the 0.22 μm filter applied, larger extracellular vesicles were removed and relatively pure conditional serum was acquired, from which blood exosomes could be purified by ultracentrifugation. Ultimately, approximately 0.18 mg of blood exosomes could be purified from 10 mL of mouse serum. As 1.0 mg blood exsosomes (by total protein quantity) is equal to around 4.16×10^{11} blood exosomes particles (Fig. 1A), 0.18 mg of blood exosomes contained about 7.49×10^{10} particles. TEM showed purified blood exosomes to be saucer shaped with sizes between 40 and 200 nm, consistent with other studies [9,11,19,20] (Fig. 1B); > 70% of all exosomes were in the range of 70–100 nm as determined by Tunable Resistive Pulse Sensing (Fig. 1A). Western blotting of exosome preparations was used to characterize blood exosomes. The results show the levels of CD9, CD63 and CD81 were positively related to the total protein levels of exosome preparations, and blood exosomes contained these exosomal marker proteins (Fig. 1C) [21].

3.2. Brain targeting by blood exosomes in vitro and in vivo

Then we studied the internalization of blood exosomes using bEnd.3 cells as a model of mouse brain endothelial cells at the BBB. Blood exosomes were labeled with the red fluorescent membrane dye PHK26 and incubated with cells for 15 min to 2 h. Cells took up different numbers of exosomes at different times, with uptake peaking at 1 h, which may be related to transcytosis of cells (a type of transcellular transports), commonly observed in brain endothelial cells (Fig. 2A and Fig. S1A) [22,23]. During transcytosis, when bEnd.3 cells take up blood exosomes, some internalized exosomes might be ejected from cells at the same time. Nevertheless, internalization of exosomes dominates in initial stage, however, exocytosis will eventually exceed internalization after the intracellular accumulation of exosomes reaching a certain degree. Hence, the 1-h time point was used in subsequent studies. Three-dimensional imaging showed that internalized blood exosomes localized to the cytoplasm and nuclei rather than adsorbing onto cellular membranes (Movie S1). To quantify exosome uptake by bEnd.3 cells, exosomes labeled with green fluorescent membrane dye PHK67 were added to cells and incubated for 1 h. The cells were then analyzed by flow cytometry (Fig. 2B). Most cells were strongly fluorescent (62.58 ± 3.36%) after incubation with blood exosomes, consistent with confocal results.

To investigate the brain targeting ability of blood exosomes *in vivo*, DiD-labeled blood exosomes were administered intravenously to nude mice, and near-infrared fluorescence images were acquired at different times (Fig. 2C). Exosomes accumulated selectively in the brain between 1 and 10 h after injection, with fluorescence intensity peaking approximately 4–8 h after injection. Subsequently, fluorescence intensity began to decline and completely disappeared by 24 h after injection. To better distinguish where exosomes localized, a birds-eye perspective of the brain from mouse atlas of MSOT in vision 128 (iThera Medical, Germany) (Fig. S1B), showing the location of the brain in a mouse, was generated. Indeed, parts of fluorescent region in Fig. 2C colocalized with certain regions of the brain (inside the rectangle in the fig. S1B). Because abundant blood flows through the carotid arteries and cerebral arteries [24] where plenty of blood exosomes exist, the overwhelmingly strong fluorescence in the brain observed *via in vivo* imaging might be partially artificial. Nontheless, *ex vivo* images of isolated brains clearly show that the DiD-labeled blood exosomes distributed in the brain (albeit weaker than the *in vivo* results, Fig. 2D and Fig. S1C), which is deprived of the disturbance of blood flow. In contrast, free DiD injected intravenously into control animals accumulated much less in the brain between 30 min and 24 h after injection, which indicates that DiD is not affecting distribution of blood exosomes, especially in brain (Fig. S1D).

3.3. Transferrin-TfR interaction for brain targeting by blood exosomes

It is known that transferrin is abundant in blood plasma [25] and it binds tightly and specifically to transferrin receptor (TfR), which is expressed at high levels on exosomes derived from blood [26,27] as well as on the surface of cerebral microvascular endothelial cells. The interaction of transferrin and TfR has already been exploited to mediate transport across the BBB *via* TfR-mediated endocytosis [28]. Thus, we hypothesized that blood exosomes could deliver drugs past the BBB based on the transferrin-TfR interaction and herein the hypothesis was verified. Indeed, western blotting revealed that TfR was abundantly expressed by bEnd.3 cells and blood exosomes, while little was expressed on human cervical cancer cell lines HeLa or exosomes derived from them (Fig. 3A). Therefore, we used HeLa exosomes as negative controls in subsequent studies. We selected exosomes from the murine bone marrow-derived dendritic cell lines DC 2.4 as a positive control because they contain high levels of TfR (Table S1). Enzyme-linked immunosorbent assay showed that transferrin was present at high levels in serum as well as blood exosomes (Table S2).

When bEnd.3 cells were pre-incubated with 40, 80 or 160 μg/mL of

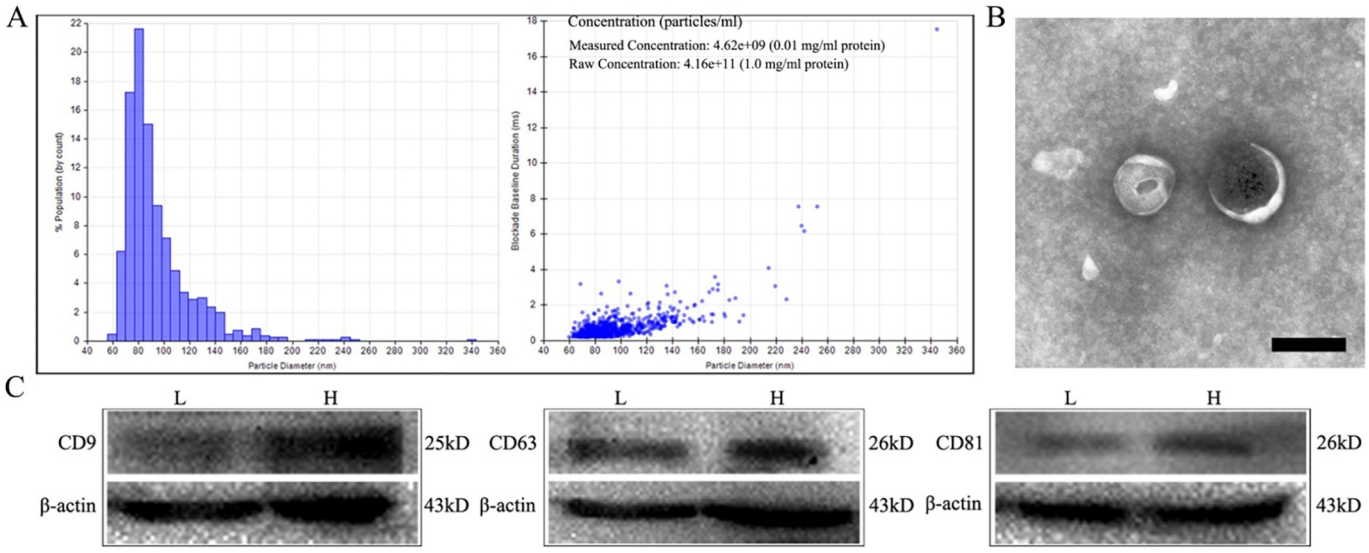

Fig. 1. Characterization of blood exosomes. (A) Distribution of exosome size and the concentration of exosomes, based on Tunable Resistive Pulse Sensing. (B) A representative TEM image. Scale bar, 100 nm. (C) Western blots of exosome preparations to confirm the expression of the exosomal marker proteins CD9, CD63 and CD81. L means exosome preparations contain a lower protein content (3.5 mg/mL); H, a higher protein content (5.0 mg/mL).

transferrin for 30 min and then mixed with PKH67-labeled blood exosomes, the uptake of exosomes was reduced in a concentration-dependent manner (Fig. 3B). This suggests that pre-treatment with free transferrin titrated TfR on bEnd.3 cells and thereby enhanced TfR internalization, reducing amount of TfR on cell-surface. Consequently, interaction with the transferrin on blood exosomes was reduced. Conversely, when blood exosomes were pre-incubated with 40, 80 or 160 μg/mL of transferrin for 4 h and then mixed with bEnd.3 cells, the uptake of exosomes increased in a concentration-dependent manner, with the greatest internalization occurring after pre-incubation with 160 μg/mL of transferrin (Fig. 3B). This increase in uptake may due to increased transferrin on blood exosomes surface (Table S2). Neither type of pre-treatment significantly altered uptake of negative-control HeLa exosomes (Fig. S2A), while results from positive-control DC 2.4 exosomes were similar to those for blood exosomes (Fig. S2B). When bEnd.3 cells were replaced with HeLa cells as the internalizing cells, uptake of exosomes was not significantly affected by pre-treatment (Fig. S2C). This provides further evidence for the importance of the transferrin-TfR interaction for brain targeting by blood exosomes. Consistently, we also found that removing surface proteins of blood exosomes using proteinase K significantly decreased exosome uptake ($P < .001$, Fig. S2D). Surface plasmon resonance studies showed that doubling the concentration of blood exosomes led to a > 2-fold increase in resonance signal, consistent with tight, specific binding between transferrin and TfR (Fig. S2E, F).

These various lines of experiments are consistent with the hypothesis that the interaction between blood exosomes and bEnd.3 cells is based on TfR-transferrin binding. To identify the probable stoichiometry of transferrin and TfR in such a complex interaction, we incubated transferrin for 4 h at 4 or 37 °C and analyzed the protein by tricine-polyacrylamide gel electrophoresis. The results are consistent with transferrin dimer (Fig. 3C). No such dimer was detected when transferrin was incubated for 4 h at 37 °C and then subjected to denaturing tricine-SDS-polyacrylamide electrophoresis (Fig. S2G). Based on these results, we performed computer modeling to simulate the binding of transferrin dimer to TfR. The ZDOCK rigid-body protein docking program was used to analyze 3600 predictions following refinement with the RDOCK algorithm. The best prediction (3S9n) was selected (Fig. 3D), which suggested the feasibility that the transferrin dimer exists and binds two TfRs to form a tetramer (Fig. 3E).

Several studies reported the cellular uptake mechanism of exosomes, but the exosome uptake mechanism is different depending on their sources. Herein, to take the first step towards identifying details about the mechanism of cellular uptake of blood exosomes, we examined the effects of energy depletion and treatment with various endocytosis inhibitors on uptake. These experiments showed that exosome uptake is energy-dependent and involves clathrin-mediated, macropinocytotic and caveolin-mediated processes (Fig. S2D).

3.4. Dopamine loading into blood exosomes and effects on dopamine-associated toxicity

Having verified the targeting ability of blood exosomes, we loaded blood exosomes with dopamine for actual PD treatment. Incubation method was employed to load dopamine here, as it is a widely used method. Here, taking account of the membrane fluidity of exosome, we modified the method by using saturated solution to improve loading efficiency. The maximum concentration difference achieved would aid dopamine passively penetrate exosomes. This method gave a loading efficiency (15.97 ± 0.22%) and proved superior to other loading methods [9–11]. Residual free dopamine was removed by ultracentrifugation. In the purified dopamine-loaded exosomes, we suggest that most of dopamine existed inside of exosomes, not associated with their membranes, because no rapid release of dopamine from dopamine-loaded blood exosomes was presented *in vitro* (Fig. S3A); the inner water phase and the lipid bilayer of exosomes may slow down the release of water-soluble dopamine. Incorporation of dopamine slightly increased average exosome size (Fig. S3B), without affecting the overall size distribution or morphology (Fig. S3C, D).

Further, we found dopamine encapsulated into blood exosomes triggered lower toxicity against the human neuroblastoma cell lines SH-SY5Y, which expresses dopaminergic markers, than free dopamine across a range of concentrations (Fig. S4A). Encapsulated dopamine did not trigger significant cell death at any concentration tested, whereas 48-h exposure to free dopamine caused significant cell death at 200 μM ($P < .05$) and 400 μM ($P < .01$; Fig. S4B). Similarly, encapsulated dopamine did not cause significant production of reactive oxygen species at any concentration tested, whereas 400 μM free dopamine did ($P < .05$; Fig. S4C). In cultures of SH-SY5Y cells, 50 μM free dopamine significantly reduced mitochondrial membrane potential ($P < .01$), which compromises mitochondrial function and cellular viability [30], but dopamine encapsulated in blood exosomes did not significantly

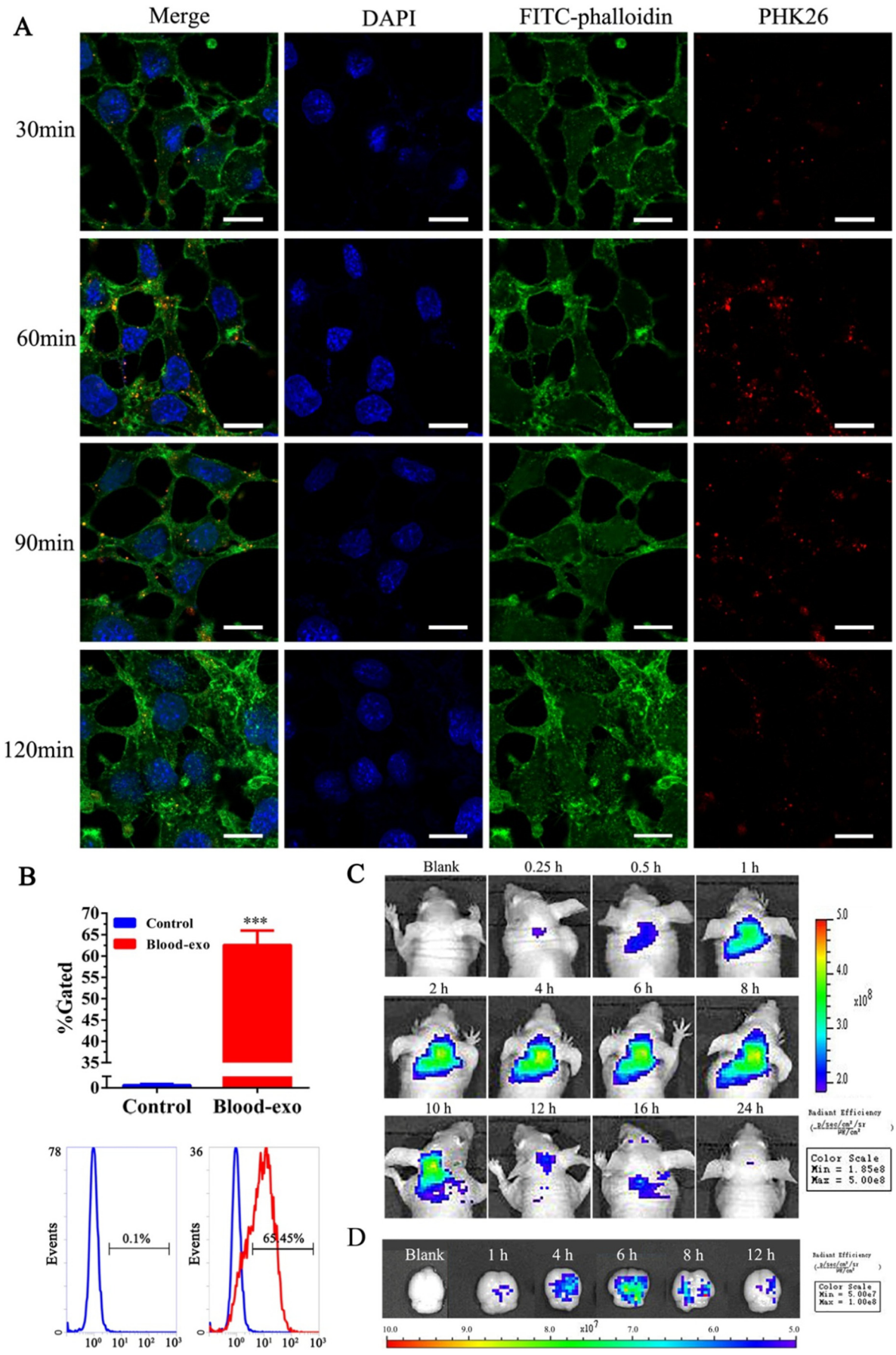

(caption on next page)

Fig. 2. Uptake of blood exosomes (blood-exo) by bEnd.3 cells in culture and *in vivo* distribution of exosomes in mice. (A) Confocal microscopy showing uptake of exosomes after incubation for 30–120 min. Exosomes appear in red; nucleus, blue; and cytoplasm, green. Scale bar, 5 μm. (B) Quantitation of exosome uptake by flow cytometry (FITC channel) after 1 h of incubation. Cells incubated with exosomes are shown in red; control cells, blue. Data shown are mean ± SD ($n = 3$). ***$P < .001$ *vs* control. (C) *In vivo* fluorescence images of nude mice at 0.25 h to 24 h after intravenous administration of DiD-labeled blood exosomes. (D) *Ex vivo* fluorescence images of isolated brains at 1 h to 12 h after intravenous administration of DiD-labeled blood exosomes. (For interpretation of the references to colour in this figure legend, the reader is referred to the web version of this article.)

reduce the membrane potential until reaching the concentration of 400 μM (Fig. S4D). Activity of tyrosine hydroxylase, which catalyzes the rate-limiting step in catecholamine synthesis, was higher in SH-SH5Y cells exposed to encapsulated dopamine than in cells exposed to the same amount of free dopamine for the same period (Fig. S4E). These data are consistent with the known ability of free dopamine to induce toxicity and increase oxidative stress [31], and they indicate that encapsulation of the drug in blood exosomes can significantly reduce its toxicity. Dopamine is released relatively slowly from blood exosomes *in vitro* (Fig. S3A), which may help explain why the exosomes reduce its toxic effects.

3.5. Brain targeting by dopamine-loaded blood exosomes in vitro and in vivo

To validate the ability of dopamine-encapsulated blood exosomes to deliver dopamine into brain, a transwell assay with bEnd.3 cells as a model of the BBB was used [32]. Cells were allowed to develop a uniform monolayer on the transwell membrane, the integrity of which was confirmed based on transendothelial electric resistance of 380 ± 8 $\Omega \cdot cm^2$ (higher than the minimum of 250 $\Omega \cdot cm^2$ for an intact membrane [33]) and based on leakage of fluorescein sodium, which was ≤40% in the presence of a bEnd.3 monolayer but > 90% in its absence (Fig. S5A). Using this BBB model, blood exosomes were found to facilitate dopamine transport across it *via* an energy-dependent mechanism that was blocked by NaN_3 or incubation at 4 °C (Fig. 4A).

Next, we analyzed the distribution of dopamine delivered as free drug or encapsulated into blood exosomes in the major organs of mice at 6 h after intravenous injection. Encapsulated dopamine was present in all major organs, including brain, to a significantly greater extent than free dopamine ($P < .001$; Fig. 4B). When delivered by blood exosomes, the dopamine concentration in the brain was 1.02 ± 0.15 nmol/g, while dopamine was not detectable in the brain from mice receiving free dopamine (the detecting limit was 0.065 nmol/g by tandem mass spectrometry). This result suggested a > 15-fold higher brain distribution of dopamine could be achieved by loading this drug into blood exosomes. Free dopamine tended to accumulate in the liver, lung and kidney, consistent with a short half-life in the body and with relatively rapid clearance/elimination [34].

Then we examined whether encapsulated dopamine could be taken up by cells in lesion areas of the brain from PD's patients, which we modelled using the dopaminergic cell lines SH-SY5Y. Many PHK67/

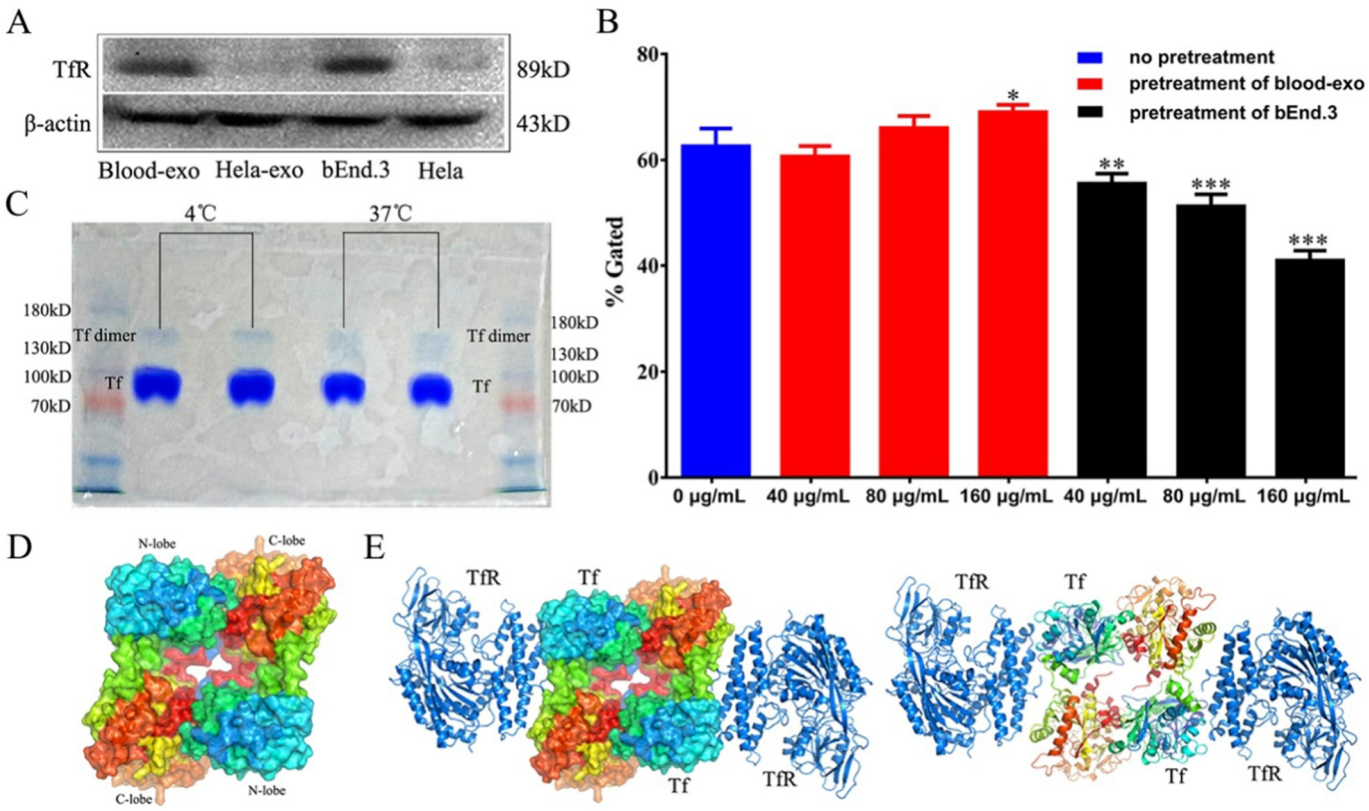

Fig. 3. Involvement of the transferrin-TfR interaction in blood exosome delivery to the brain. (A) Expression of TfR on exosomes prepared from mouse blood (blood-exo) or HeLa cells (Hela-exo), and on bEnd.3 cells or HeLa cells. (B) Uptake of blood exosomes by bEnd.3 cells following pre-treatment with increasing amounts of transferrin. Blue indicates that blood exosomes and bEnd.3 cells were mixed without any pre-treatment; red, that exosomes were pre-treated with transferrin; and black, that bEnd.3 cells were pre-treated with transferrin. Data shown are mean ± SD ($n = 3$). *$P < .05$, **$P < .01$, ***$P < .001$ *vs* 0 μg/mL. (C) Confirmation of transferrin (Tf) dimer in phosphate buffer solution based on tricine-polyacrylamide. (D) ZDOCK prediction of the structure of the transferrin dimer, based on structural models of transferrin and TfR [29]. (E) Tetramer of transferrin dimer and two TfRs predicted by ZDOCK, shown as transferrin molecules in surface (left) and ribbon (right) representations. (For interpretation of the references to colour in this figure legend, the reader is referred to the web version of this article.)

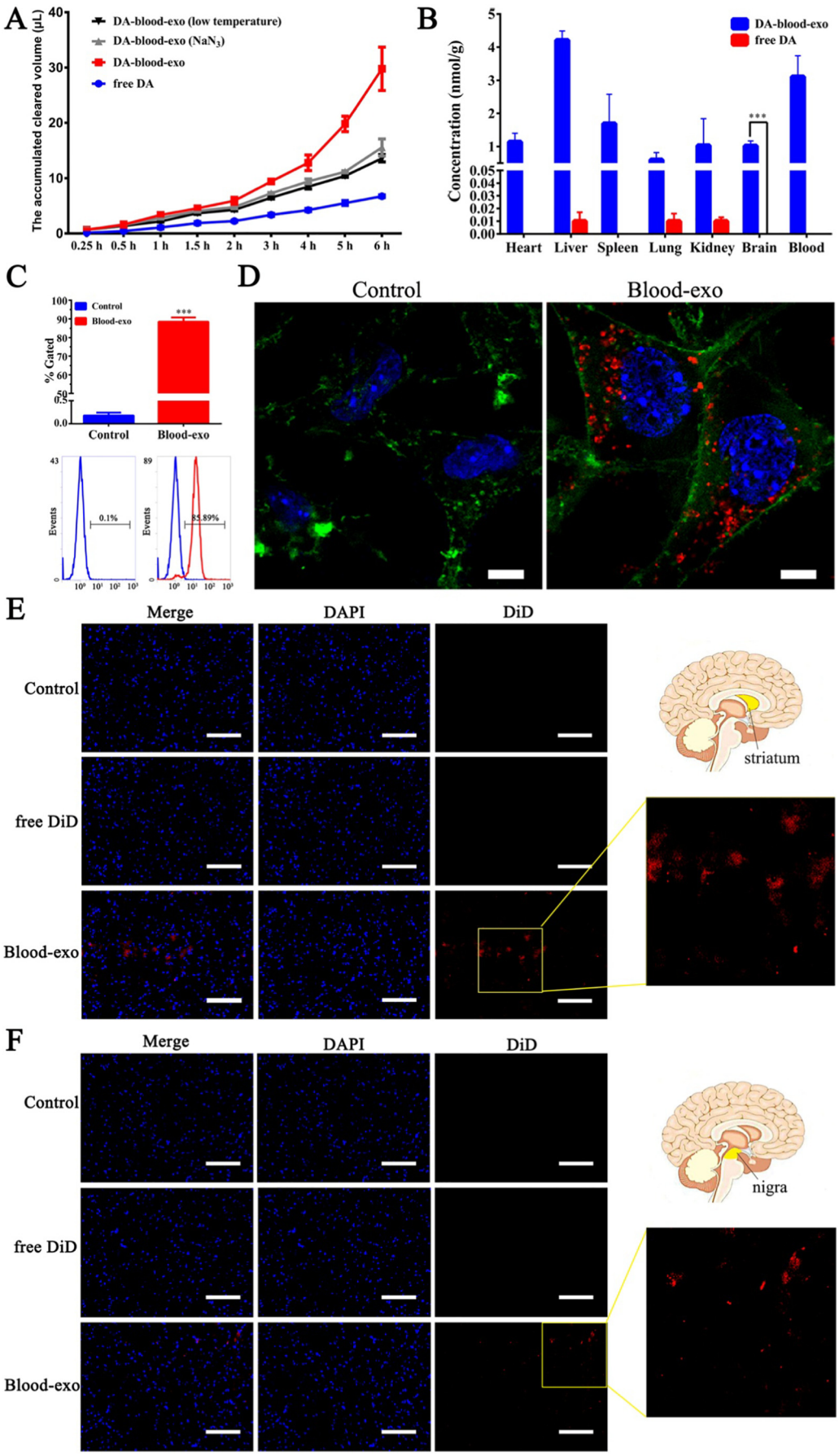

Fig. 4. Brain targeting of dopamine-loaded blood exosomes *in vitro* and *in vivo*. (A) Accumulated cleared volume across an *in vitro* BBB model following treatment with free dopamine or dopamine-loaded blood exosomes in the presence or absence of NaN_3 and at 37 °C or 4 °C. (B) Dopamine distribution in mouse organs at 6 h after intravenous injection. Data shown are mean ± SD ($n = 5$). *** $P < .001$. (C) Uptake of blood exosomes by SH-SY5Y cells after 1-h incubation using flow cytometry (FITC channel). Cells incubated with exosomes are shown in red; control cells, in blue. Data shown are mean ± SD ($n = 3$). ***P < .001 *vs* control. (D) Uptake of blood exosomes by SH-SY5Y cells after 1-h incubation using confocal microscopy. Blood exosomes are shown in red; nucleus, blue; and cytoplasm, green. Scale bar, 2 μm. Fluorescence images of (E) striatum and (F) substantia nigra in brain sections obtained after mice were intravenously injected with free DiD or DiD-labeled blood exosomes. DA, dopamine; blood-exo, blood exosomes; DA-blood-exo, dopamine-loaded blood exosomes. Scale bar, 100 μm. (For interpretation of the references to colour in this figure legend, the reader is referred to the web version of this article.)

PHK26-labeled exosomes were internalized by these cells in culture as determined by flow cytometry and confocal microscopy (Fig. 4C, D). This uptake was found to be energy-dependent and involves clathrin, macropinocytosis and caveolin pathways (Fig. S5B), which is the same as in bEnd.3 cells. The results showed blood exosomes could get into the dopaminergic neurons.

In separate experiments, mice were intravenously injected with DiD-labeled blood exosomes and at 6 h later the brains were removed and sectioned. Exosomes were observed in the striatum and substantia nigra (Fig. 4E, F), which were the lesion areas for treating PD [35], suggesting blood exosomes could get into the lesion regions. In addition, exosomes were found in the hippocampus (Fig. S5C).

3.6. Therapeutic efficacy of dopamine-loaded blood exosomes against PD

For further investigation of the therapeutic efficacy, dopamine-loaded blood exosomes were systemically administered to a mouse model of PD. Among the published rat and mouse models of PD, administrating 6-hydroxydopamine (6-OHDA), 1-methyl-4-phenyl-1,2,3,6-tetrahydropyridine or rotenone are well established [36,37]. We selected the Kunming mouse injected with 6-OHDA model because of its stability and our previous experiences with these mice using exosomes. In this study, 6-OHDA was administered directly into the medial forebrain bundle, and the pathological features of the 6-OHDA-lesioned PD mouse model were illustrated in the Fig. 5A. We established this model, and confirmed the PD phenotype based on both behavioral imbalance (ipsiversive rotation ratio $>$ 95%) and both loss of striatal dopamine ($>$ 80%) and reduced tyrosine hydroxylase activity in the lesioned striatum (Fig. S6).

These mice were randomly divided into 5 groups treated for 3 weeks with one of the following: sterile 0.9% saline (negative control), unloaded blood exosomes, free levodopa (positive control), free dopamine, or dopamine-loaded blood exosomes. A group of healthy animals (sham control) was administered and treated with sterile 0.9% saline. Behavioral imbalance (ipsiversive rotation) assessment was carried out to study the effects of these treatments on neurobehavioral function in mouse with PD. A significant decrease in amphetamine-induced rotations was observed in the animals treated with dopamine-loaded exosomes ($P < .01$) and levodopa ($P < .05$) when compared to 6-OHDA-lesioned mouse (Fig. S7). In contrast, only minor decreases of rotational scores were measured in animals treated with blood exosomes amd dopamine. In addition, because supplementary of dopamine could induce endogenous nigral dopaminergic neurogenesis, loss-of-function effects would be improved, including producing endogenous dopamine and several functional enzymes catalyzing catecholamine synthesis or against oxidative stress (Fig. 5A) [38]. Thus, these relevant indexes were also investigated to evaluate the therapeutic effect. Compared with negative control, the amount of dopamine in lesioned striatum of animals treated with dopamine-loaded exosomes increased significantly ($P < .001$) and was 56.58% higher than that in sham controls. There was only slight improvement in animals treated with levodopa ($P < .05$) or free dopamine ($P < .01$), compared with animals treated with dopamine-loaded exosomes (Fig. 5B). Levels of tyrosine hydroxylase in lesioned striatum, which were lower in negative controls than in sham controls, was improved more by dopamine-loaded exosomes treatment than by levodopa treatment (Fig. 5C). Free dopamine, in contrast, did not significantly alter enzyme levels. Saline-treated animals showed lower striatal levels of glutathione, superoxide dismutase and catalase than sham controls, as well as lower total antioxidant capacity in striatum ($P < .001$, Fig. 5D-G). However, all four parameters were greatly increased after the dopamine-loaded exosomes treatment, which were much higher than that after the treatment with levodopa or free dopamine. Besides, unloaded blood exosomes showed no obvious therapeutic efficacy against PD (Fig. 5B-G). These results all suggested that dopamine-loaded blood exosomes can help improve dopaminergic neurons and ameliorate disease phenotype in a mouse model of PD.

3.7. In vivo toxicity of dopamine-loaded blood exosomes

Since our experiments above indicated the presence of dopamine-loaded blood exosomes in non-lesion areas within the brain (hippocampus) and outside the brain (heart, liver, spleen, lung and kidney), we examined the strength of toxic effects. Our results show that dopamine-loaded exosomes did not cause evident histopathology in hippocampus (Fig. S8A), liver, spleen or lung (Fig. S8B). Free dopamine triggered clear inflammatory cell infiltration in the heart, whereas dopamine-loaded exosomes did not (Fig. S8B). Animals treated with these exosomes also showed normal values of biomarkers for heart function (creatine kinase [39]), liver function (aspartate aminotransferase, alanine aminotransferase [40]) and kidney function (urea nitrogen, serum creatinine [41]) (Table S3). On the other hand, dopamine-loaded exosomes did cause detectable mesangiolysis to a similar extent as free dopamine (Fig. S8B), which may due to the breakdown of exosomes and subsequent release of dopamine in kidney.

All together, these results suggested that blood exosomes show promise as a safe brain-targeting drug delivery system.

4. Conclusion

In the current study, for the first time, we showed blood exosomes without any modification could serve as efficient carriers for brain targeted delivery of drugs and we also revealed the underlying mechanism for their natural distribution to the brain. We next took full use of dopamine-loaded blood exosomes for targeted therapy against PD, preferably solving the unmet medical need of treating PD.

Herein, we validated the primary hypothesis that blood exosomes could deliver drugs past the BBB based on the transferrin-TfR interaction on the prerequisite of the existence of transferrin dimer. We supposed that drug-loaded exosomes would have a great chance to bind to transferrin receptors and get into the brain, although there might be a concern that large numbers of empty exosomes in the blood maybe saturate transferrin receptors in the BBB, hence the binding and transcellular transport of drug-loaded exosomes to the brain would be impeded. It is known that the interaction between transferrin and TfR is a dynamic endocytic cycle: transferrin binds to TfR on the cell surface and the complexes are internalized; after the iron is released, transferrin without iron lefts the receptor and then the receptor returns to the cell surface for the next cycle [29]. Similarly, we suggest that the binding, transport and delivery of blood exosomes is also a dynamic endocytic cycle, which is mediated by transferrin and TfR. Therefore, enough TfR should be available for drug-loaded exosomes to bind. This hypothesis is supported by our animal experiments.

In addition, it is well known that extracellular vesicles (EVs) mainly include two core categories: exosomes and microvesicles, which could be preliminarily distinguished according to their size-range [6]. Taking account of the measured sizes of vesicles in our study and the fact that reticulocytes-released extracellular membrane vesicles have been defined as “exosomes” in 1983 [42], we identified these dominantly reticulocytes-originated vesicles as blood exosomes.

According to our calculation, blood exosomes showing natural brain targeting ability are abundant in blood, which is reasonably easy to acquire. It is reported that around 2×10^{11} aged erythrocytes are replaced every day in human (*i.e.* about 2×10^{6} reticulocytes mature every second) [43,44]. We therefore estimate that about 10^{14} exosomes are released by reticulocytes in the bloodstream every day. The quantities of other common cells in the blood that produces exosomes (mainly including white blood cells (4–10) $\times 10^{4}$/μL [45] and blood platelets (1–3) $\times 10^{5}$/μL [46]) are much smaller than erythrocytes, not to mention cells from organs. They also generate much fewer exosomes daily per cell. Hence, compared with reticulocytes, much fewer exosomes could be generated from other cells in the blood, which means

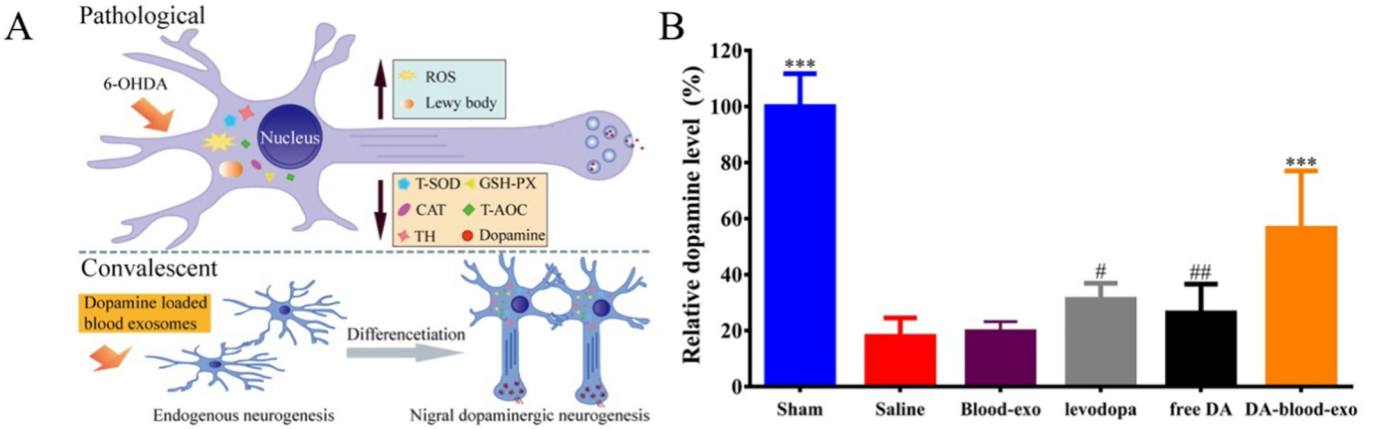

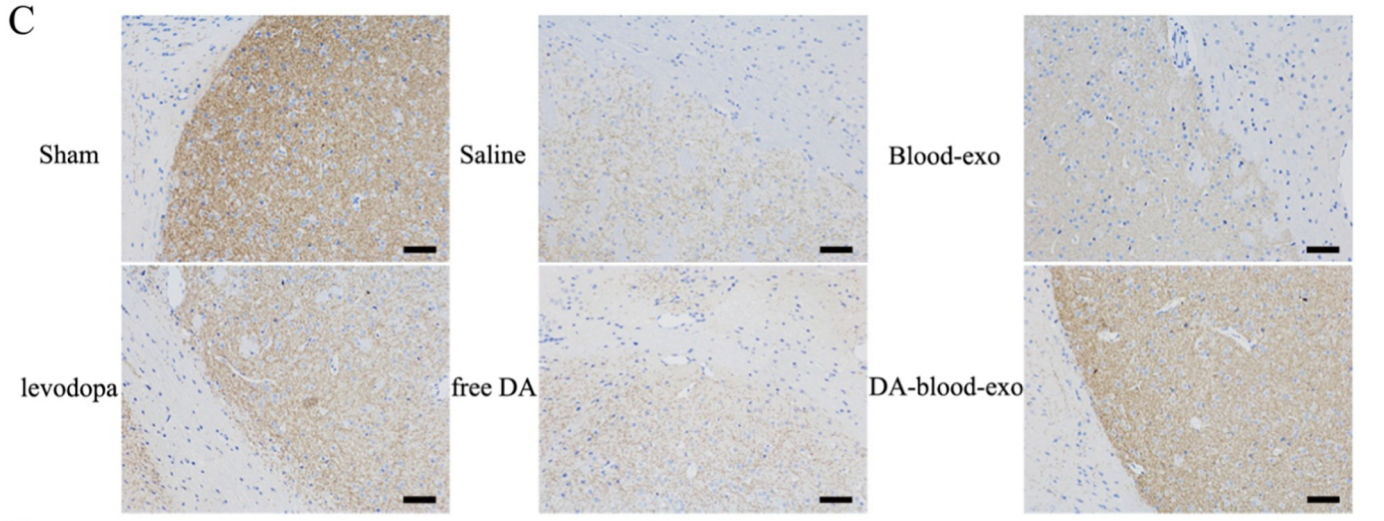

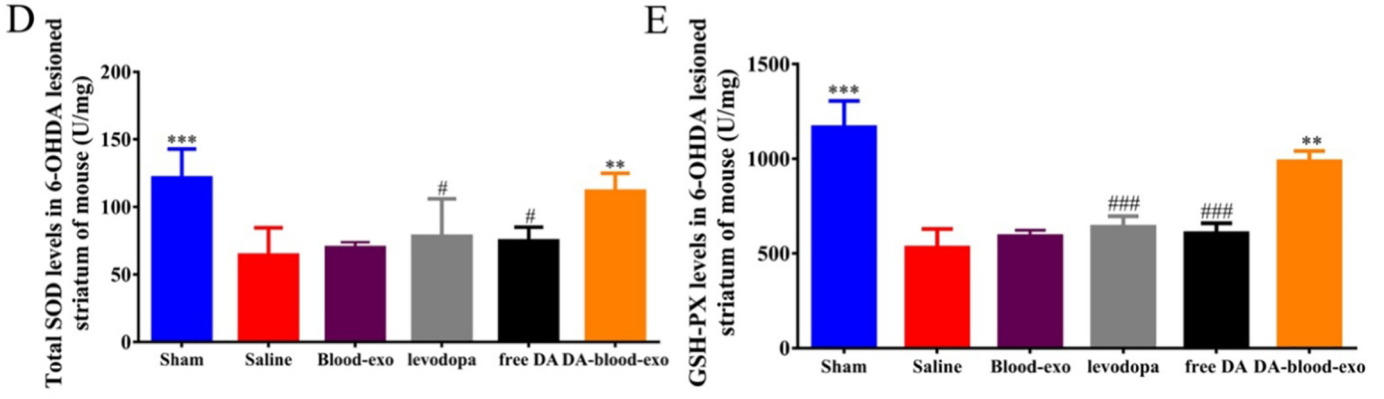

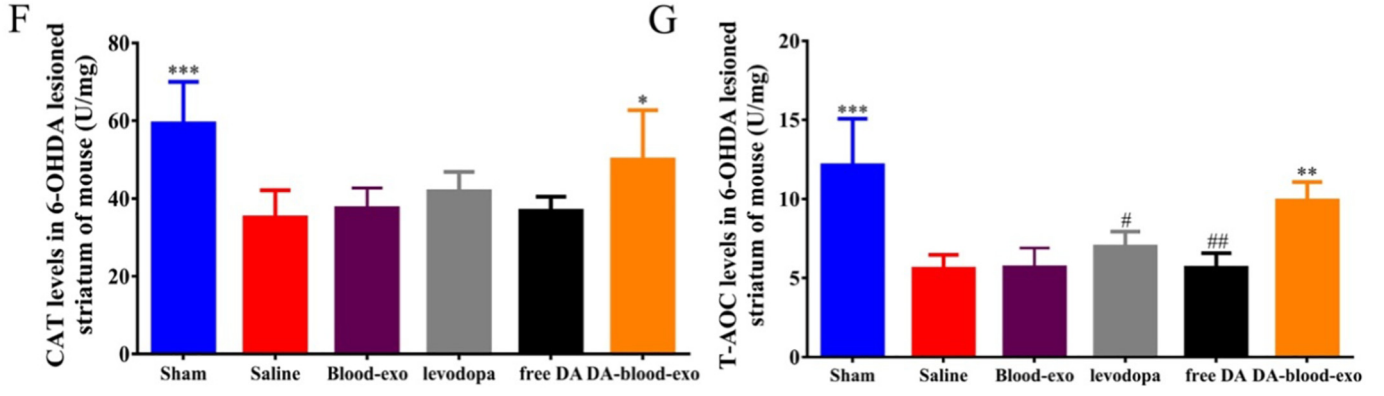

(caption on next page)

Fig. 5. Therapeutic effects of free dopamine (DA) and dopamine encapsulated in blood exosomes (DA-blood-exo) in a mouse model of PD. Effects were measured in the striatum at 3 weeks after 6-OHDA administration. Sham control animals were treated with sterile 0.9% saline. (A) The pathological features of the 6-OHDA-lesioned PD mouse model and the process of neurogenesis. (B) Relative dopamine level compared with sham control animals. (C) Tyrosine hydroxylase immunoreactivity. Scale bar, 70 μm. (D) Total SOD levels. (E) Levels of GSH-PX. (F) Levels of CAT. (G) T-AOC levels. Data shown are mean ± SD ($n = 5$). $^{*}P < .05$, $^{**}P < .01$, $^{***}P < .001$ *vs* saline-treated animals; $^{\#}P < .05$, $^{\#\#}P < .01$, $^{\#\#\#}P < .001$ *vs* DA-blood-exo treated animals. Blood-exo means unloaded blood exosomes; T-SOD means total superoxide dismutase; GSH-PX, glutathione peroxidase; CAT, catalase; T-AOC, total antioxidant capacity; TH, tyrosine hydroxylase.

blood-born exosomes are predominantly produced by reticulocytes.

As described, dopamine-encapsulated blood exosomes successfully delivered dopamine into brain, striatum and substantia nigra. After a period of treatment, the slow-released supplementary of dopamine could induce endogenous nigral dopaminergic neurogenesis; then these neurons could produce endogenous dopamine and several functional enzymes, improving the symptomatic performance of PD's patients [38]. Thus, beside of behavioral performance, we also examined the levels of striatum dopamine and relative enzymes (including tyrosine hydroxylase and several enzymes against oxidative stress) in most studies to indirectly evaluate the therapeutic effect. Evidences from different aspects all show that dopamine-loaded blood exosomes could indeed improve disease phenotype in a mouse model of PD.

In summary, we have constructed and validated, *in vitro* and *in vivo*, a blood exosome system for delivering drugs to the brain through the BBB. We have demonstrated significant therapeutic effects by loading the exosomes with dopamine and systemically injecting them into a mouse model of PD. In addition to the strong therapeutic efficacy, the exosomes also significantly reduced the systemic toxicity associated with free dopamine. The ability of blood exosomes to pass through the BBB and be taken up by brain cells appears to involve strong, specific interactions between transferrin and TfR. Computer modeling suggests the possibility that transferrin dimer in the blood simultaneously interact with two TfRs, one on the exosome and the other on the target cell.

Our findings prove that blood exosomes are power carriers for brain-targeting therapy against PD and potentially for other diseases of the central nervous system too.

Supplementary data to this article can be found online at https://doi.org/10.1016/j.jconrel.2018.08.035.

Competing interests

The authors declare that they have no competing interests.

Acknowledgements

This work was supported by the National Natural Science Foundation of China [grant numbers 81690261] and the Graduate Student's Research and Innovation Fund of Sichuan University. We thank Prof. Jianxin Wang and M.S. Zhonglian Cao from school of pharmacy, Fudan University for surface plasmon resonance assessment. Really appreciate Dr. P Luo of Izon Science Europe Ltd to provide Tunable Resistive Pulse Sensing.

References

[1] C.S. Nicholas J Kassebaum, Christopher J L Murray, Alan D Lopez, and Rafael Lozano, Global, regional, and national levels of maternal mortality, 1990–2015: a systematic analysis for the Global Burden of Disease Study 2015, Lancet, 388 (2016) 1775–1812.
[2] V.L.D. Ted, M. Dawson, Molecular pathways of neurodegeneration in Parkinson's disease, Science 302 (2003) 819–822.
[3] A.Y.O. Mine Silindir Gunay, Sylvie Chalon, Drug delivery systems for imaging and therapy of Parkinson's disease, Curr. Neuropharmacol. 14 (2016) 376–391.
[4] P. Huot, T.H. Johnston, J.B. Koprich, S.H. Fox, J.M. Brotchie, The pharmacology of L-DOPA-induced dyskinesia in Parkinson's disease, Pharmacol. Rev. 65 (2013) 171–222.
[5] P.C. Hiroto Kuwabara, Yoshifumi Yasuhara, Gabriel C. Leger, Mark Guttman, Mirko Diksic, Alan C. Evans, Albert Gjedde, Regional striatal DOPA transport and decarboxylase activity in Parkinson's disease, J. Nucl. Med. 36 (1995) 1226–1231.
[6] D. Ingato, J.U. Lee, S.J. Sim, Y.J. Kwon, Good things come in small packages: Overcoming challenges to harness extracellular vesicles for therapeutic delivery, J. Control. Release 241 (2016) 174–185.
[7] S.L.S. Sean, D. Conner, Regulated portals of entry into the cell, Nature 422 (2003) 37–44.
[8] J.M.G. Kasper, Bendix Johnsen, Martin Najbjerg Skov, Linda Pilgaard, Torben Moos, Meg Duroux, A comprehensive overview of exosomes as drug delivery vehicles - endogenous nanocarriers for targeted cancer therapy, Biochim. Biophys. Acta 1846 (2014) 75–87.
[9] S.L. Yanhua Tian, Jian Song, Tianjiao Ji, Motao Zhua, Gregory J. Anderson, Jingyan Wei, Guangjun Nie, A doxorubicin delivery platform using engineered natural membrane vesicle exosomes for targeted tumor therapy, Biomaterials 35 (2014) 2383–2390.
[10] M.J.H. Myung Soo Kim, Yuling Zhao, Vivek Mahajan, Irina Dey-Gen, Natalia L. Klyachko, Eli Inskoe, Aleksandr Piroyan, Marina Sokolsky, Onyi Okolie, Shawn D. Hingtgen, Alexander V. Kabanov, Elena V. Batrakova, Development of exosome-encapsulated paclitaxel to overcome MDR in cancer cells, Nanomedicine 12 (2016) 655–664.
[11] X.Z. Dongmei Sun, Xiaoyu Xiang, Yuelong Liu, Shuangyin Zhang, Cunren Liu, Stephen Barnes, William Grizzle, Donald Miller, Huang-Ge Zhang, A novel nanoparticle drug delivery system: the anti-inflammatory activity of curcumin is enhanced when encapsulated in exosomes, Mol. Therapy 18 (2010) 1606–1614.
[12] M.T. Shin-Ichiro Ohno, Katsuko Sudo, Shinobu Ueda, Akio Ishikawa, Nagahisa Matsuyama, Koji Fujita, Takayuki Mizutani, Tadaaki Ohgi, Takahiro Ochiya, Noriko Gotoh, Masahiko Kuroda, Systemically injected exosomes targeted to EGFR deliver antitumor MicroRNA to breast cancer cells, Mol. Ther. 21 (2013) 185–191.
[13] D.-j.Y. Jung-Ah Cho, Hye-Youn Son, Hyun-Wha Kim, Dae-Sun Jung, Jae-Kyun Ko, Jason Soonju Koh, Yong-Nyun Kim, Chul-Woo Kim, Exosomes: a new delivery system for tumor antigens in cancer immunotherapy, Int. J. Cancer 114 (2005) 613–622.
[14] Y.S. Lydia Alvarez-Erviti, HaiFang Yin, Corinne Betts, Samira Lakhal, Matthew J.A. Wood, Delivery of siRNA to the mouse brain by systemic injection of targeted exosomes, Nat. Biotechnol. 29 (2011) 341–345.
[15] R. Kojima, D. Bojar, G. Rizzi, G.C. Hamri, M.D. El-Baba, P. Saxena, S. Auslander, K.R. Tan, M. Fussenegger, Designer exosomes produced by implanted cells intracerebrally deliver therapeutic cargo for Parkinson's disease treatment, Nat. Commun. 9 (2018) 1305.
[16] X.X. Xiaoying Zhuang, William Grizzle, Dongmei Sun, Shuangqin Zhang, Robert C. Axtell, Songwen Ju, Jiangyao Mu, Lifeng Zhang, Lawrence Steinman, Donald Miller and Huang-Ge Zhang, Treatment of brain inflammatory diseases by delivering exosome encapsulated anti-inflammatory drugs from the nasal region to the brain, Mol. Ther. 19 (2011) 1769–1779.
[17] J.S.-M. Michel Vidal, Jean R. Philippot, Alain Bienvenue, Asymmetric distribution of phospholipids in the membrane of vesicles released during in vitro maturation of guinea pig reticulocytes: evidence precluding a role for "aminophospholipid translocase", J. Cell. Physiol. 140 (1989) 455–462.
[18] Y. Li, Y. Zhou, B. Qi, T. Gong, X. Sun, Y. Fu, Z. Zhang, Brain-specific delivery of dopamine mediated by n,n-dimethyl amino group for the treatment of Parkinson's disease, Mol. Pharm. 11 (2014) 3174–3185.
[19] H. Peinado, M. Aleckovic, S. Lavotshkin, I. Matei, B. Costa-Silva, G. Moreno-Bueno, M. Hergueta-Redondo, C. Williams, G. Garcia-Santos, C. Ghajar, A. Nitadori-Hoshino, C. Hoffman, K. Badal, B.A. Garcia, M.K. Callahan, J. Yuan, V.R. Martins, J. Skog, R.N. Kaplan, M.S. Brady, J.D. Wolchok, P.B. Chapman, Y. Kang, J. Bromberg, D. Lyden, Melanoma exosomes educate bone marrow progenitor cells toward a pro-metastatic phenotype through MET, Nat. Med. 18 (2012) 883–891.
[20] D. Zabeo, A. Cvjetkovic, C. Lasser, M. Schorb, J. Lotvall, J.L. Hoog, Exosomes purified from a single cell type have diverse morphology, J. Extracellular Vesicles 6 (2017) 1329476.
[21] R. Wubbolts, R.S. Leckie, P.T. Veenhuizen, G. Schwarzmann, W. Mobius, J. Hoernschemeyer, J.W. Slot, H.J. Geuze, W. Stoorvogel, Proteomic and biochemical analyses of human B cell-derived exosomes. Potential implications for their function and multivesicular body formation, J. Biol. Chem. 278 (2003) 10963–10972.
[22] D.A.G.a.N.J.S. Stuart K. Williams, Endocytosis and exocytosis of protein in capillary endothelium, J. Cell. Physiol. 120 (1984) 157–162.
[23] J.B.R.J.B. Fishman, J.V. Handrahan, J.R. Connor, R.E. Fine, Receptor-mediated transcytosis of transferrin across the blood-brain barrier, J. Neurosci. Res. 18 (1987) 299–304.
[24] W. Contributors, Cerebral Circulation, in, Wikipedia, the Free Encyclopedia, https://en.wikipedia.org/w/index.php?title=Cerebral_circulation&oldid=790359983, (2017).
[25] J.C.M. Catherine Nicholls, Distribution of six Tf C (Transferrin) subtypes in cord bloods and blood donors, J. Exp. Biol. Med. Sci. 60 (1982) 433–436.
[26] C.L. Hongzhao Qi, Lixia Long, Yu Ren, Shanshan Zhang, Xiaodan Chang, Xiaomin Qian, Huanhuan Jia, Jin Zhao, Jinjin Sun, Xin Hou, Xubo Yuan, Chunsheng Kang, Blood exosomes endowed with magnetic and targeting properties

for cancer therapy, ACS Nano 10 (2016) 3323–3333.
[27] R.M.J. Bin-Tao Pan, Fate of the transferrin receptor during maturation of sheep reticulocytes in vitro: selective externalization of the receptor, Cell 33 (1983) 967–977.
[28] H.L. Zhong Ming Qian, Hongzhe Sun, Kwokping Ho, Targeted drug delivery via the transferrin receptor-mediated endocytosis pathway, Pharmacol. Rev. 54 (4) (2002) 561–587.
[29] A.N.S. Brian E. Eckenroth, N. Dennis Chasteen, Stephen J. Everse, Anne B. Mason, How the binding of human transferrin primes the transferrin receptor potentiating iron release at endosomal pH, PNAS 108 (2011) 13089–13094.
[30] G.A. Alexander, V. Zhdanov, Ulla G. Knaus, Dmitri B. Papkovsky, Cellular ROS imaging with hydro-Cy3 dye is strongly influenced by mitochondrial membrane potential, Biochim. Biophys. Acta 1861 (2017) 198–204.
[31] I.M.a.N.O. Masato Asanuma, Dopamine- or L-DOPA-induced neurotoxicity: the role of dopamine quinone formation and tyrosinase in a model of Parkinson's disease, Neurotox. Res. 5 (3) (2003) 165–176.
[32] H. Gao, Z. Yang, S. Zhang, Z. Pang, Q. Liu, X. Jiang, Study and evaluation of mechanisms of dual targeting drug delivery system with tumor microenvironment assays compared with normal assays, Acta Biomater. 10 (2014) 858–867.
[33] S. Nakagawa, M.A. Deli, H. Kawaguchi, T. Shimizudani, T. Shimono, A. Kittel, K. Tanaka, M. Niwa, A new blood-brain barrier model using primary rat brain endothelial cells, pericytes and astrocytes, Neurochem. Int. 54 (2009) 253–263.
[34] P.H.S. Maher K. Eldadah, Richard Harrison, Christopher J.L. Newth, Pharmacokinetics of dopamine in infants and children, Crit. Care Med. 19 (1991) 1008–1011.
[35] M. Velázquez-Paniagua, A.M. Vázquez-Álvarez, G. Valverde-Aguilar, P. Vergara-Aragón, Current treatments in Parkinson's including the proposal of an innovative dopamine microimplant, Rev. Méd. Hospit. Gen. México 79 (2016) 79–87.
[36] B.M. Shane Grealish, Peter Draxler, Anders Bjorklund, Characterisation of behavioural and neurodegenerative changes induced by intranigral 6-hydroxydopamine lesions in a mouse model of Parkinson's disease, Eur. J. Neurosci. 31 (2010) 2266–2278.
[37] A.M.F. Amira, M. Solimana, Ahmed A. Moustafa, Dose-dependent neuroprotective effect of caffeine on a rotenone-induced rat model of parkinsonism: a histological study, Neurosci. Lett. 623 (2016) 63–70.
[38] A.B.a.G.U. Hoglinger, Dopamine and adult neurogenesis, J. Neurochem. 100 (2007) 587–595.
[39] R.V.-C.V.A. Saks, Z.A. Huchua, A.N. Preobrazhensky, I.V. Emelin, Creatine kinase in regulation of heart function and metabolism, Biochim. Btophys. Acta 803 (1984) 254–264.
[40] B. Miguel, Practical guidelines for examination of adults with asymptomatic hypertransaminasaemia, Gastroenterol. Hepatol. (English Edition) 40 (2017) 99–106.
[41] G.-D.Z. Yan-Ling Zhao, Hong-Bo Yang, Jia-Bo Wang, Li-Mei Shan, Rui-sheng Li, Xiao-He Xiao, Rhein protects against acetaminophen-induced hepatic and renal toxicity, Food Chem. Toxicol. 49 (2011) 1705–1710.
[42] C.V. Harding, J.E. Heuser, P.D. Stahl, Exosomes: looking back three decades and into the future, J. Cell Biol. 200 (2013) 367–371.
[43] J.A. Blom, Monitoring of Respiration and Circulation, CRC Press, Boca Raton London New York Washington, D.C., 2003.
[44] A.D.G. Lionel Blanc, Ge'minard Charles, Pascale Bette-Bobillo, Michel Vidal, Exosome release by reticulocytes—an integral part of the red blood cell differentiation system, Blood Cells Mol. Dis. 35 (2005) 21–26.
[45] Vital and Health Statistics National Center for Health Statistics, Hyattsville, Maryland, 2005.
[46] L.H.A. Dennis, W. Ross, Judith Watson, A. Stuart, Bentley stability of hematologic parameters in healthy subjects, Am. J. Clin. Pathol. 90 (1988) 262–267.